12 Jan 87 Conference Presentation

Visualization of Unsteady Separated Flow About a Pitching Delta Wing

TA 2307-F1-38

F. Gilliam, J. Wissler, M. Robinson, J. Walker

F.J. Seiler Research Laboratory
USAF Academy CO 80840-6528

FJSRL-PR-90-0006



Distribution Unlimited

Unsteady separated flows produced by three different delta wings driven with constant pitch rates were investigated using high speed flow visualization. The large scale vortices produced were initially similar to those produced above delta wings driven sinusoidally. Subsequently, the vortices either convected away from the wing or were broken up by the complex three-dimensional flow field. Both initiation and development of the leading edge vortices were dependent upon planform geometry and nondimensional pitch rate. Variations in vortex characteristics and duration with spanwise position were also noted. Smoke wire visualization proved a valuable tool in assessing the three-dimensional characteristics of the unsteady flow field.

flow visualization
flow separation
delta wings

13

UNCLASSIFIED UNCLASSIFIED UNCLASSIFIED NONE

AIAA'87



# AIAA-87-0240
# Visualization of Unsteady Separated Flow About a Pitching Delta Wing

F. Gilliam, J. Wissler,
Dept. of Aeronautics, USAF Academy, Co.
M. Robinson,
Dept. of Aerospace Engr. Sci.,
Univ. of Colorado, Boulder, Co.
J. Walker,
Frank J. Seiler Research Laboratory,
USAF Academy, Co.



**AIAA 25th Aerospace Sciences Meeting**
January 12-15, 1987/Reno, Nevada

# VISUALIZATION OF UNSTEADY SEPARATED FLOW ABOUT A PITCHING DELTA WING

F.T. Gilliam
J.B. Wissler
Dept of Aeronautics
U.S. Air Force Academy

M.C. Robinson
Dept of Aerospace Engineering
University of Colorado

J.M. Walker
Frank J. Seiler Research Laboratory
U.S. Air Force Academy

## Abstract

Unsteady separated flows produced by three different delta wings driven with constant pitch rates were investigated using high speed flow visualization. The large scale vortices produced were initially similar to those produced above delta wings driven sinusoidally. Subsequently, the vortices either convected away from the wing or were broken up by the complex three-dimensional flow field. Both initiation and development of the leading edge vortices were dependent upon planform geometry and nondimensional pitch rate. Variations in vortex characteristics and duration with spanwise position were also noted. Smoke wire visualization proved a valuable tool in assessing the three-dimensional characteristics of the unsteady flow field.

## Nomenclature

| | |
|---|---|
| $c_r$ | wing root chord |
| $t$ | time |
| $t$ | nondimensional time $tV_\infty/c_r$ |
| $V_\infty$ | freestream velocity |
| $\alpha$ | angle of attack |
| $\dot{\alpha}$ | pitch rate |
| $\dot{\alpha}^+$ | nondimensional pitch rate |
| $\Lambda$ | leading edge wing sweep |

* Lt Col, USAF, Associate Professor, Member AIAA
** Capt, USAF, Instructor, Member AIAA
*** Associate Professor Adjunct, Currently Visiting Professor, United States Air Force Academy, Member AIAA
**** Maj, USAF, Chief, Aeromechanics Division, FJSRL, Member AIAA



## Introduction

The large transient forces produced through forced unsteady fllow separation have been well documented over a variety of test models and flow conditions. (1-13) The large scale vortices derived from the forced flow separation are both reproducible and, to some extent, controllable. (14,15) Hence, many utilization schemes have been envisioned (13,16) to exploit unsteady aerodynamics in order to enhance conventional airfoil performance. Most of these efforts have focused upon control of the large scale vortices in two-dimensional test conditions because of the inherent complexities involved in a three-dimensional, unsteady, separated flow environment. (17,18,19,20,22) As yet, neither the basic processes driving vortex development in the two-dimensional case nor the applicability of two-dimensional results to three-dimensional configurations are well understood.

The flow field about a three-dimensional pitching wing is substantially more complicated than similar flows about two-dimensional airfoils. (17,18,19,20) Unsteady separation over a two-dimensional airfoil is dominated by the initiation and development of a leading edge vortex which rapidly increases in diameter while convecting over the airfoil surface. (1-13,15,21) In contrast, the three-dimensional flow about a finite straight wing is further complicated by the addition of an unsteady wing tip vortex and orthogonal vortex-vortex interactions between the wing tip and inboard leading edge vortices. (17,19,20)

Previous experiments on pitching straight wings (17,19,20) showed three distinct regions of flow field development. The wing tip vortex dominated the flow field near the tip, the dynamic stall or leading edge vortex, dominated the flow field on the upper wing surface away from the tip, and an interaction region was apparent between the two sites of organized vorticity. The flow visualization results of Adler and Luttges (17) were obtained for a straight wing undergoing low amplitude sinusoidal pitching motions, and the dynamic stall vortices were found to dominate the

flow field in the region inboard of a position approximately one chord length from the wing tip. Experiments by Robinson, et al, (20) of a straight wing undergoing high constant pitch rate, high amplitude motion histories found the interaction region to be larger, persisting to a position that was 1.4 chord lengths inboard from the tip. In both three-dimensional cases though, the dynamic stall vortex appeared to dominate the flow field in regions sufficiently far removed from the wing tip vortex in much the same manner as found in two-dimensional experiments.

Flow about an unsteady delta wing is even more complex with a three-dimensional geometry eliciting unsteady vortices with geometry dependent initial alignments. Gad-el Hak and Ho (18,22) found that for a delta wing pitching sinusoidally, the leading edge vortex began at the tip of the wing during the upstroke and moved inboard as the pitching motion continued. The vortex did not convect downstream, as had occurred in two-dimensional experiments, but was stationary on the wing and aligned with the wing's leading edge. The sinusoidal pitching motion sustained a growth and decay cycle in the stationary leading edge vortex. The stationary character of the unsteady leading edge vortex was not unlike the leading edge vortices found above delta wings in steady flow. Additionally, steady flow leading edge vortices have a very similar formation mechanism to dynamic stall leading edge vortices seen in this and previous experiments. In the steady flow case, flow separates around the leading edge of the wing at moderate angles of attack, and a vortex is developed parallel to and just behind the leading edge on the upper surface of the wing. Spanwise flow within the rolled up vortex is toward the wing tip. The flow impinges on the wing, reattaches, and moves forward on the wing upper surface until it separates again along a secondary separation line. This separated flow vortical structure is a primary lift-producing mechanism for delta wings in steady flow and is effective to angles of attack of $30^{o}$ or more.

This investigation examined the flow field about a delta wing pitched from zero to 60 degrees at constant pitch rates. The experiment used simple motion histories to enable a detailed understanding of the unsteady flow field development and thus provide a clear picture of the basic physics underlying the generation of the observed flow structures. Three-dimensional distortions of the flow were examined as a function of delta planform, pitch rate, and span location over the wing. These findings were compared with previous results for two-dimensional wings driven with constant pitch rates and with delta wings undergoing oscillatory motions. (15,18,22)

## Methods

Experiments were conducted in the University of Colorado's 2' x 2' low turbulence ( 0.03%) wind tunnel. Free stream velocities were set with a reference pitot tube located in the test section. One side of the tunnel was refitted with a glass wall to permit flow visualization.

Delta wings of 30, 45, and 60 degree sweep angles were used in the experiments. The wings were constructed from flat plates and had sharpened leading and trailing edges. The pitch axis was perpendicular to the freestream direction and was located at 25% of the root chord for the 30 and 45 degree delta wings. Due to potential wall impingement problems at 60 degrees angle of attack, the pitch axis was located at the 50% chord position for the 60 degree delta wing.

Fundamental to the visualization process was the delivery of a dense smoke sheet at selectable span locations. A smoke wire was constructed of 0.005 inch diameter tungsten wire and located 18" upstream of the delta wing. The wire was coated with a thin film of theatrical fogging fluid which vaporized when heated by an applied voltage. Smoke density and duration were optimized by adjusting the voltage across the wire. The smoke wire stretched 18" across the tunnel perpendicular to both the flow direction and the pitch axis. The ends of the smoke wire attached to two 0.25" diameter copper rods which were slid into and out of the test section in order to deliver a planar layer of smoke at the desired spanwise locations.

High speed motion pictures documented the dynamics of the vortex development from two separate, orthogonal vantage points. A 16 mm Locam II variable speed movie camera was operated at a frame speed of 200 frames per second. Eastman 4-X negative 16 mm movie film was exposed via a 50 mm Nikon lens set at an aperature of 2.8. Illumination was provided by two Strobrite stroboscopic flash units synchronized with the high speed camera. The single point source bulbs operated with a total duration of 7 microseconds and provided virtually instantaneous visualizations even at the highest pitch rates used.

A programmable wing motion control system drove a d.c. stepping motor through a constant pitch rate movement from 0 to 60 degrees. A 4 to 1 gear reduction between the stepper motor and the pitch shaft provided a smooth ramp function. The rotation rates used for this experiment are shown in Table 1 and correspond to nondimensional pitch rates of 0.2, 0.6, and 1.0. The freestream velocity of 10 ft/s resulted in Reynolds numbers of 25900, 43500, and 71300 respectively for the 30, 45 and 60 degree delta wings.

The motion pictures were analyzed both qualitatively and quantitatively. From a qualitative point of view, the pictures provided information on the general flow structure, and the influence of wing geometry, pitch rate, and smoke location. The quantitative analysis was obtained by digitizing select portions of the movie sequences. These digitized points included wing angle of attack at vortex initiation and the non-dimensional time at which a coherent vortex was no longer identifiable. Also, vortex position and size were tracked as a function of time. These

Table 1. Pitch Rates (deg/s) and Root Chord (in)

| wing | 30 | 45 | 60 |
|---|---|---|---|
| 0.2 | 225 | 141 | 82 |
| 0.6 | 677 | 423 | 245 |
| 1.0 | 1125 | 705 | 409 |
| root chord | 6.1 | 10.25 | 16.8 |

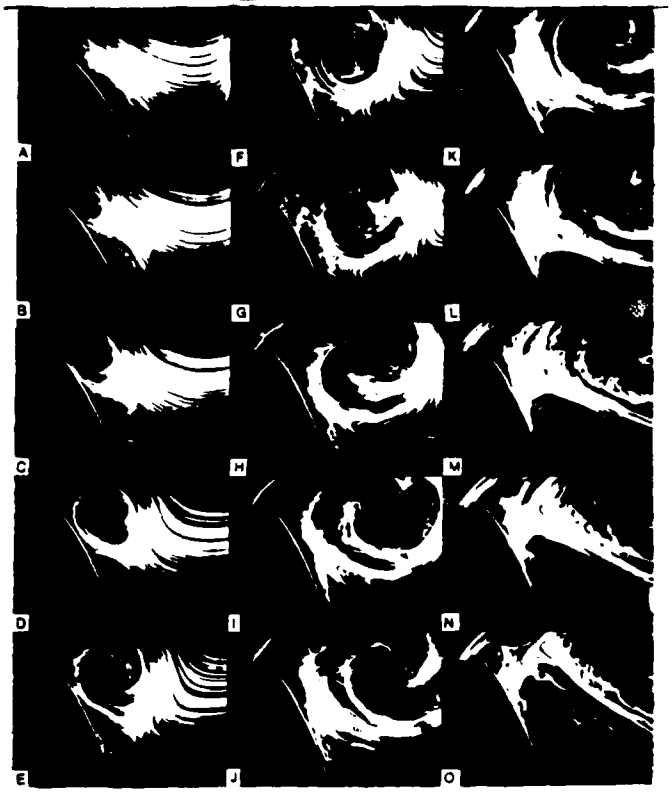


Fig. 1 - Vortex initiation over a two-dimensional wing; NACA 0015; $\alpha^{+}$ 0.6; $\Delta\bar{t}$ 0.2; $t_A$ = 1.5.

data were then plotted to reveal trends in vortex appearance, size, convection, and decay as influenced by wing planform and pitching parameters. Due to the different pitch axis used with the $\alpha = 60^{o}$ wing, the flow visualization results were not quantified at that wing sweep. It should be noted that much of the quantitative data (particularly the point at which vortex breakdown was determined) is based on very subjective evaluations of the flow field and should be regarded as useful for establishing trends, but rather imprecise in an absolute sense.

## Results

The results include a general description of the flow field about pitching delta wings as influenced by wing planform, an evaluation of flow field variations along the span of the wing, and an assessment of nondimensional pitch rate effects. Measurements of vortex initiation angle, vortex size and duration are also presented. Comparisons with straight wing results and previous delta wing experiments are used to develop a better overall appreciation of the cause and effect relationship between planform and pitch parameters and the observed flow field response. Also, some appropriate comparisons with steady flow over delta wings were used to contrast unsteady effects. Span locations were nondimensionalized by the root chord of the wing and referenced to the delta wing tip. For example, a span location of 1.0 is the spanwise station located $1.0c_r$ inboard of the wing tip.

### General Flow Structure

The flow field about a rapidly pitching two-dimensional airfoil is dominated by the dynamic stall vortex on the upper surface of the wing. Previous work by several authors (1-12) have shown this vortex to be an important mechanism in unsteady lift enhancement. The flow field about a pitching two-dimensional airfoil is shown in Figure 1, and the dynamic stall vortex is very apparent.

Vortical presence over a delta wing in steady flow produces lift in a similar manner. (18,22) These steady leading edge vortices were clearly seen in static tests of the wings used in this experiment, particularly for the $\alpha = 60^{o}$ wing. Hence, the flow field about a pitching delta wing was expected to result from the combined influences of the vorticity produced by steady and unsteady mechanisms.

The dominant flow characteristic of each wing tested was a relatively large scale vortex that developed on the wing upper surface. In some cases the vortex resembled the dynamic stall vortex seen in Figure 1, and in other cases the resemblance was similar to the leading edge vortex found over delta wings in steady flow. As noted by Gad-el-Hak and Ho (18) for oscillating motion histories, the sweep angle of the leading edge of the delta wing determined the orientation of the vortical structure. Selected photographic sequences will be used to illustrate some of the findings.

The side view of the flow field developed over a $30^{o}$ delta wing is seen in Figure 2. The pictures are selected frames from the high speed movie that recorded the flow field development. The flow direction is from left to right and the strobe lighting was directed upstream from a position behind the delta wing. The nondimensional pitch rate is 1.0, and the span location of the smoke plane is sufficiently far inboard that tip effects are minimized ($0.8c_r$ inboard of tip). Photograph A corresponds to the movie frame immediately prior to wing motion. Subsequent frames were selected such that the change in nondimensional time (nondimensionalized on root chord and freestream velocity) between frames is 0.2. The delta wing achieves $60^{o}$ angle of attack shortly after photograph F at a nondimensional time of 1.05.

The flow field in Figure 2 is not dissimilar to the two-dimensional pitching airfoil seen in Figure 1. The upper surface flow field is dominated by a vortex that initiates along the delta wing's leading edge during the pitching motion and convects back over the wing surface. However, the vortex occurs much earlier in the pitching motion for the delta wing, and the ultimate size of the developed vortex is smaller. Also, the vortex above the delta wing breaks down much earlier than for the two-dimensional airfoil. In Figure 1, the vortex is very influential until at least photograph 1L ($\bar{t} \approx 3.7$). For the delta wing case, the vortex has become very disorganized and apparently ineffective by photograph 2H ($\bar{t}$ = 1.4). The vortex is twisted by three dimensional effects that change the flow field from very coherent to very chaotic. The flow field seen in photographs 2H through 2J contrasts dramatically

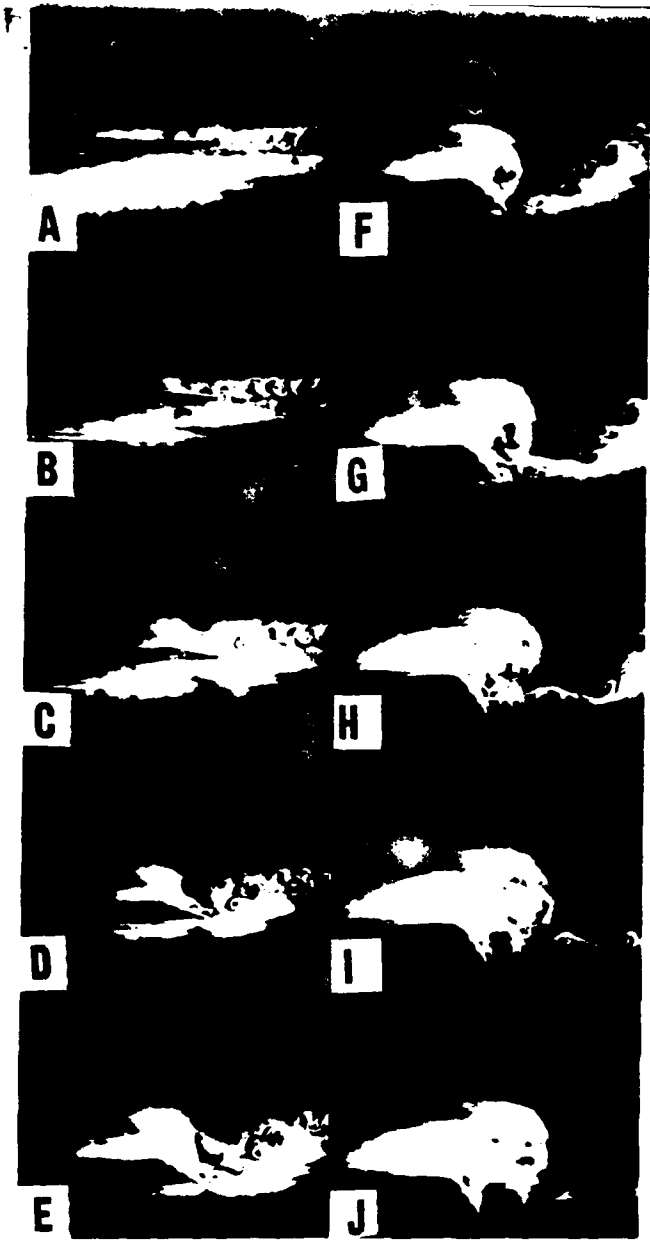


Fig. 2 - $\Lambda 30^{\circ}$; $\alpha^{+} 1.0$; $c_r$ 0.8; $\Delta\bar{t}$ 0.2;

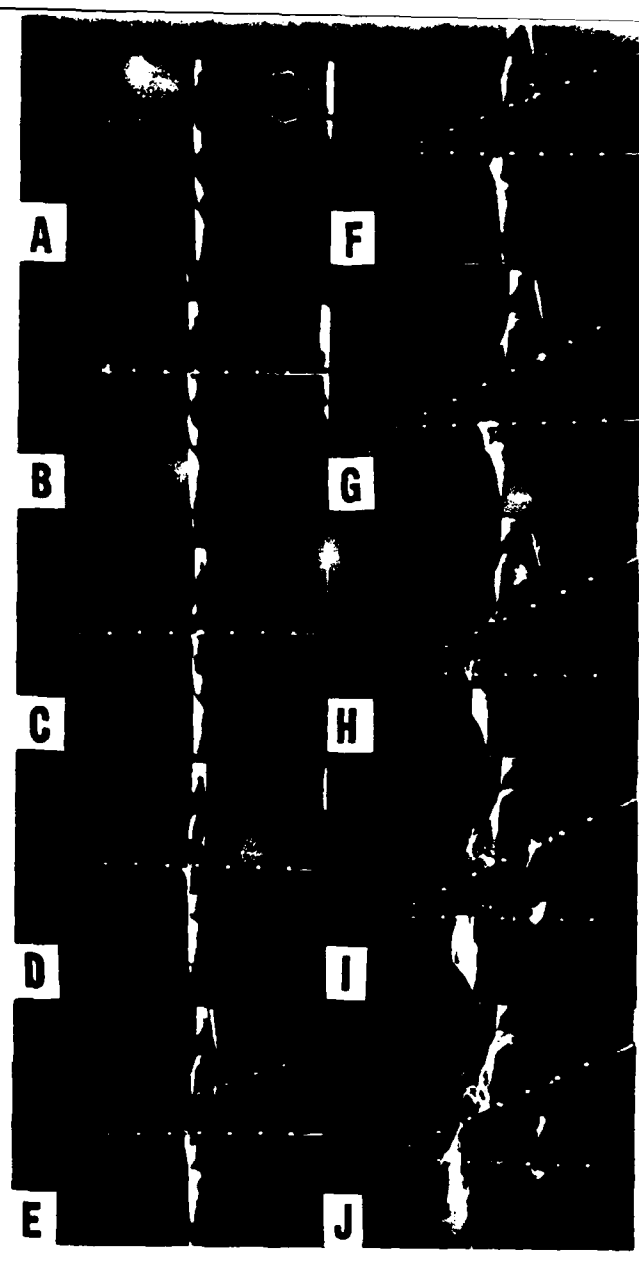


Fig. 3 - $\Lambda 30^{\circ}$; $\alpha^{+} 1.0$; $c_r$ 0.8; $\Delta\bar{t}$ 0.2;

with the remarkably coherent leading edge vortex and smooth smoke streaklines that persist well past the $60^{\circ}$ point for the two-dimensional airfoil.

When the same pitching delta wing is viewed from a vantage point behind the wing, three-dimensional distortion of the flow field is readily apparent. The planar sheet of smoke (coming toward the reader) approaches the wing at a span position $0.8c_r$ inboard from the wing tip. White reference tic marks on the wing trailing edge were evenly spaced at a distance of $0.2c_r$. The smoke sheet remained reasonably planar as the wing pitching motion began until the leading edge vortex formed (photograph 3C). Subsequently, the sheet of smoke was twisted out of plane, apparently due to the twisting of the vortex line itself.

Effect of Wing Planform

The flow field about the delta wing was radically changed by planform effects, in particular, the sweep angle of the leading edge. Figures 4 and 5 show the flow field side views for the $45^{\circ}$ and $60^{\circ}$ delta wings. The non-dimensional pitch rate for both figures was 1.0 with a $\Delta\bar{t}$ between plates of 0.2. Hence, side views of the 30, 45, and 60 degree delta wings can be compared directly, plate for plate. Figures 4 and 5 show that vortex initiation for these wing sweeps occured early in the pitching motion. The vortex is clearly present in photograph 5C ( $\bar{t} = 0.4$, $\alpha = 15^{\circ}$). However, the subsequent development of the vortices for these wing sweeps is very different from that observed in the $30^{\circ}$ case.

The effects of planform on initial vortex alignment appeared to simplify the translation of the vortex from a position parallel to the leading edge to a path that is more in line with the freestream velocity vector. This smoother translation may contribute to the extended period of coherent vortical flow for the $60^{\circ}$ wing as compared to the $30^{\circ}$ wing. For the $60^{\circ}$ delta

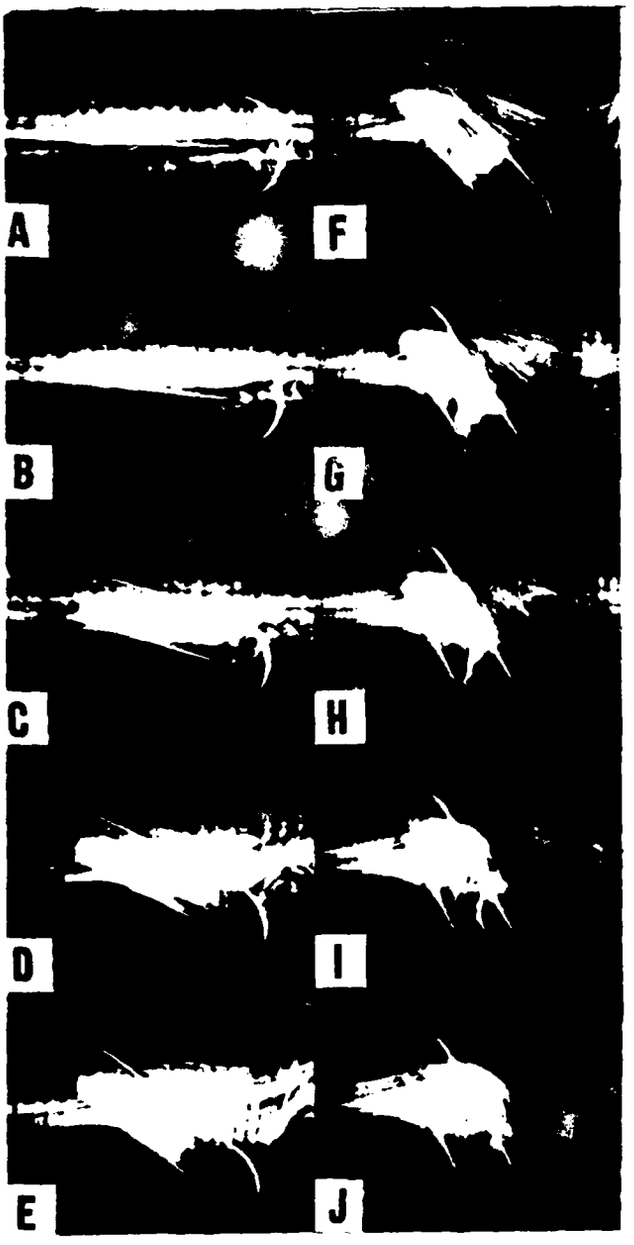


Fig. 4 - $\Lambda 45^{\circ}$; $\alpha^{+} 1.0$; $c_r$ 0.8; $\Delta\bar{t}$ 0.2;

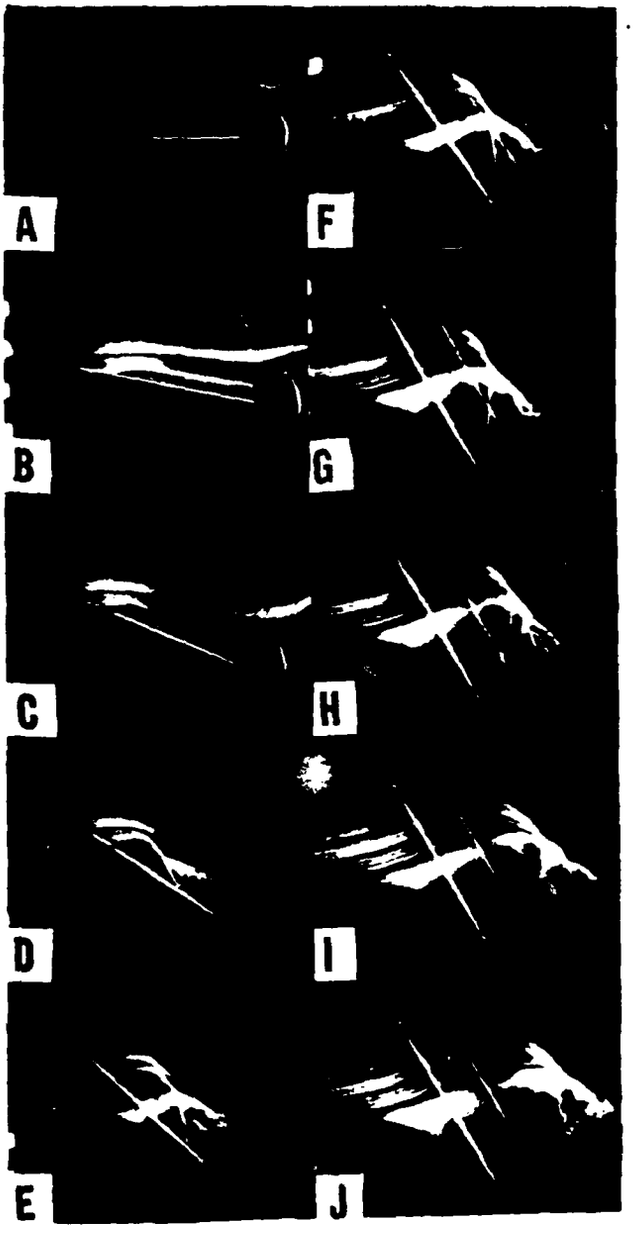


Fig. 5 - $\Lambda 60^{\circ}$; $\alpha^{+} 1.0$; $c_r$ 0.3; $\Delta\bar{t}$ 0.2;

(Figure 5), the leading edge vortex does not break down as seen in Figure 2, but apparently remains laminar until it eventually lifts off the wing and is convected downstream. The break up of the leading edge vortex in the 30° case (Figure 2H) resembles the break up seen on finite straight wings (20) which was apparently due to the orthogonal vorticity fields generated by the leading edge vortex and the wing tip vortex. As the sweep angle of the delta wing is increased, the potential for orthogonal or nearly orthogonal vortex-vortex interactions is decreased. The absence of the strong mixing caused by orthogonal vortex-vortex interactions may explain the persistence of laminar flow in the leading edge vortex above the 45° and 60° delta wings.

The aft views of Figures 4 and 5 are shown in Figures 6 and 7. These views also show the distinct difference in vortex development and spanwise flow with increasing delta angle. For the 30° delta wing (Figure 3), the vortex initiated along the leading edge in plates B-F. At later times, the vortex leaves its position parallel to the leading edge near the tip and moves left to right in that region, aligning with the velocity vector. This movement is coincident with the vortex breakdown that can be seen in the side view (photograph 2H). A similar movement occurs for the 45° (Figure 6) and 60° (Figure 7) delta wings, but is not nearly as obvious because of the initial vortex alignment being much closer to the freestream velocity. This phenomena will be examined in more detail later.

## Effect of Spanwise Location

Spanwise movement of the smoke wire enabled various selected freestream planes to be stained ahead of the wing. Several smoke wire positions were then used for each wing/motion history combination to better visualize the entire flow field about the wing. Figures 8 and 9 show the side and rear views of an identical pitching event

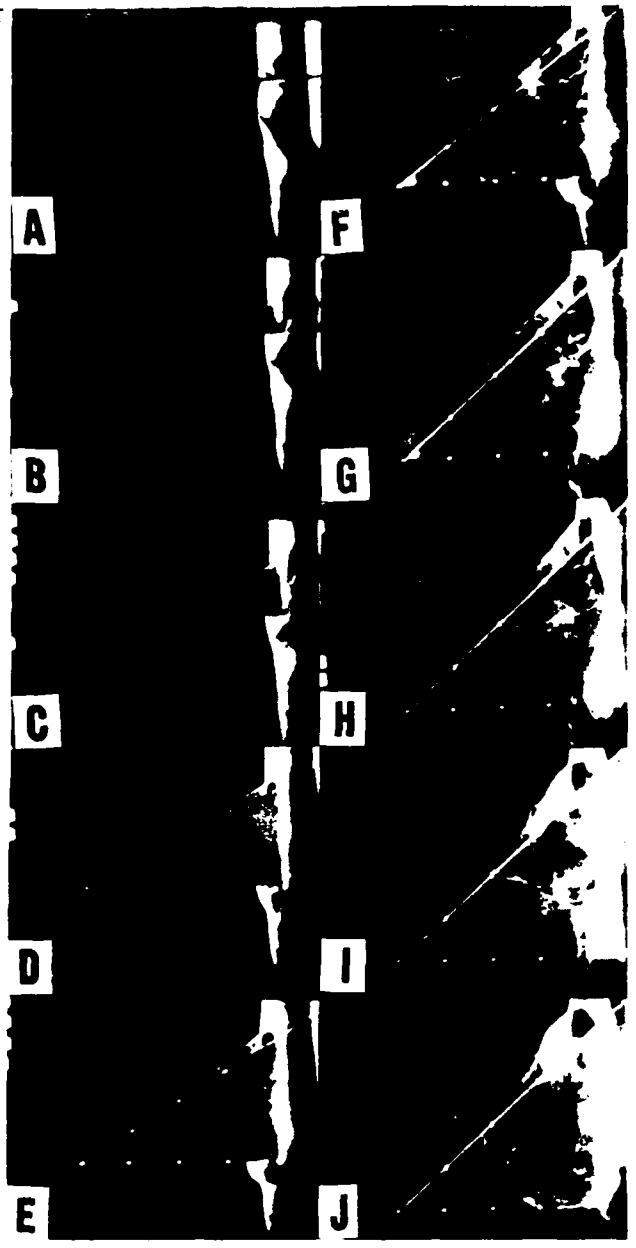


Fig. 6 - $\Lambda 45^{\circ}$; $\alpha^{+} 1.0$; $c_r$ 0.8; $\Delta\bar{t}$ 0.2;

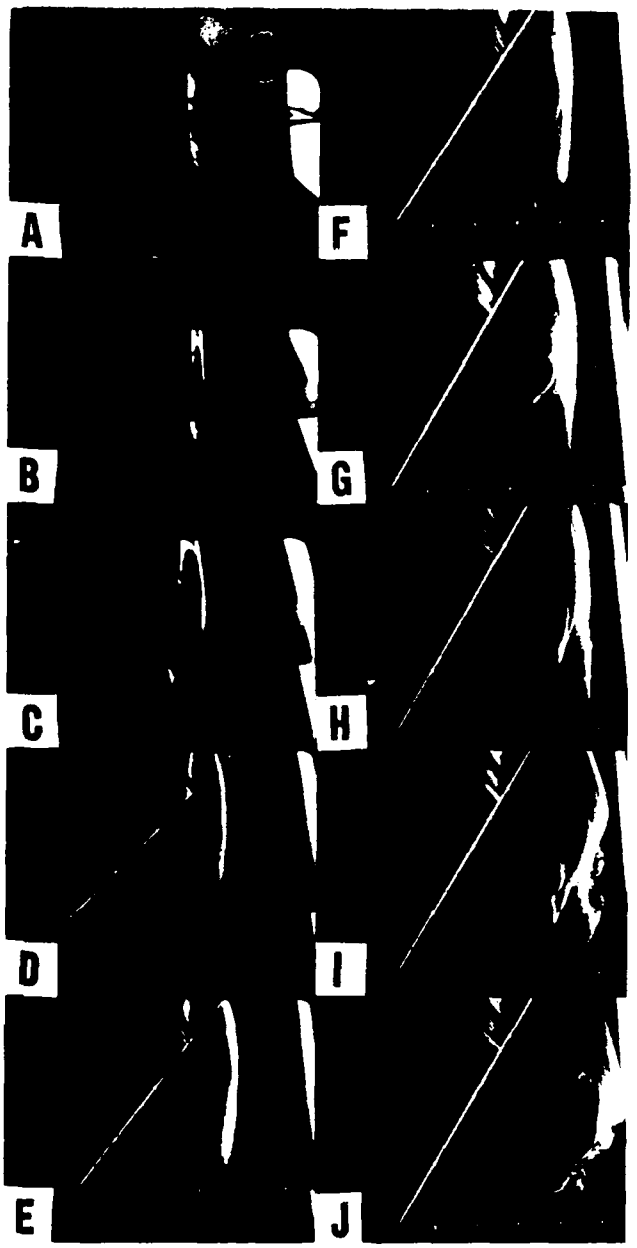


Fig. 7 - $\Lambda 60^{\circ}$; $\alpha^{+} 1.0$; $c_r$ 0.3; $\Delta\bar{t}$ 0.2;

as seen in Figures 2 and 3 ( $\alpha = 30^{\circ}$, $\alpha^{+} = 1.0$), with the smoke plane introduced at a spanwise location of $0.4c_r$.

A comparison of these photographic sequences shows several interesting phenomena. The pattern of vortices that shed into the wake during pitch up are much more regular and better formed at the inboard location (Fig 2) than at the outboard location (Fig 8). Also, the leading edge vortex developed earlier at a position near the tip than at the inboard location. This pattern would be consistent with the findings of Gad-el-Hak and Ho (18) who noticed that for sinusoidally pitching delta wings, the leading edge vortex initially developed at the wing tip during the upstroke, and then appeared along the leading edge at sucessively further inboard stations as the upstroke continued.

The persistence of the leading edge vortex is also a function of spanwise station. The vortex seen in Figure 2 at the inboard location is clearly apparent until photograph 2G ($\bar{t} = 1.2$) while the vortex at the outboard position begins to break up earlier as seen in photograph 8F ($\bar{t} = 1.0$). Once again, this behavior is very similar to the observations made for similar tests on a straight wing, where vortex-vortex interactions between nearly orthogonal vortical structures caused the earlier demise of the vortex near the wing tip. In general, vortex duration was greater at inboard positions for all nondimensional pitch rates and sweep angles. In some cases the duration was dramatically higher inboard; in other cases the difference was marginal.

Figure 8 again shows the translation of the leading edge vortex near the tip of the $30^{\circ}$ delta wing. In plots E through J, the vortex moves left to right toward the root chord. This effect appeared to be a function of wing geometry and was very noticeable for all pitch rates with the $30^{\circ}$ delta.

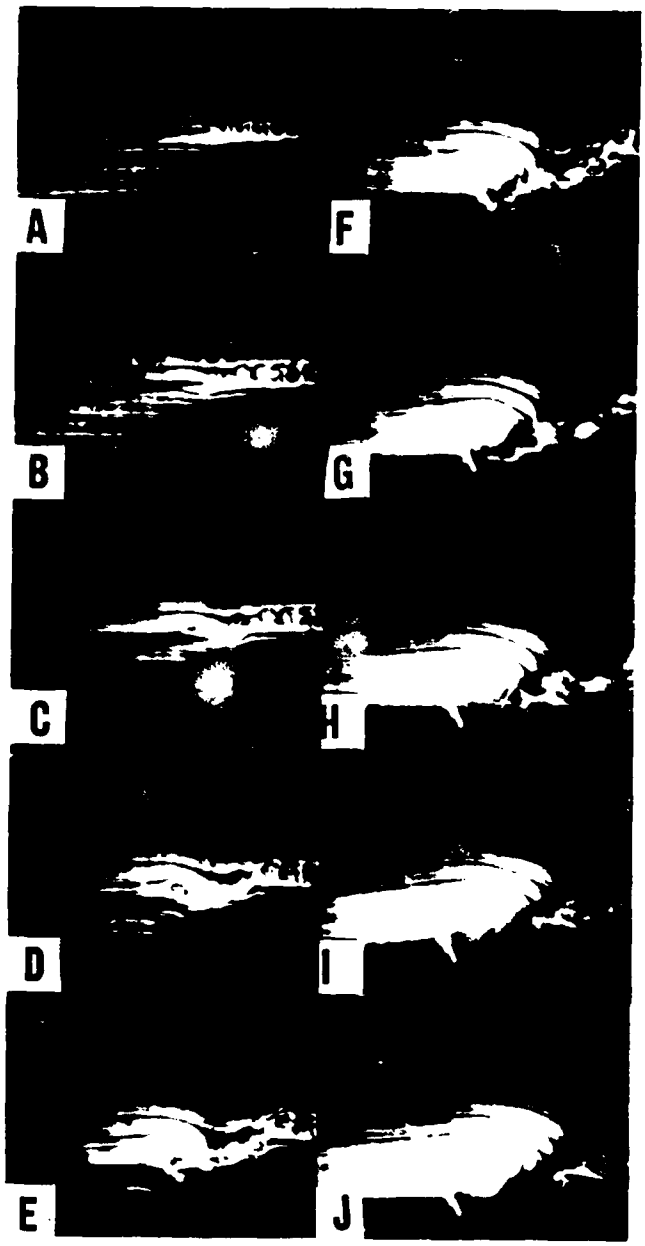


Fig. 8 - $\Lambda 30^{\circ}$; $\alpha^{+}$1.0; $c_r$ 0.4; $\Delta\bar{\epsilon}$ 0.2;

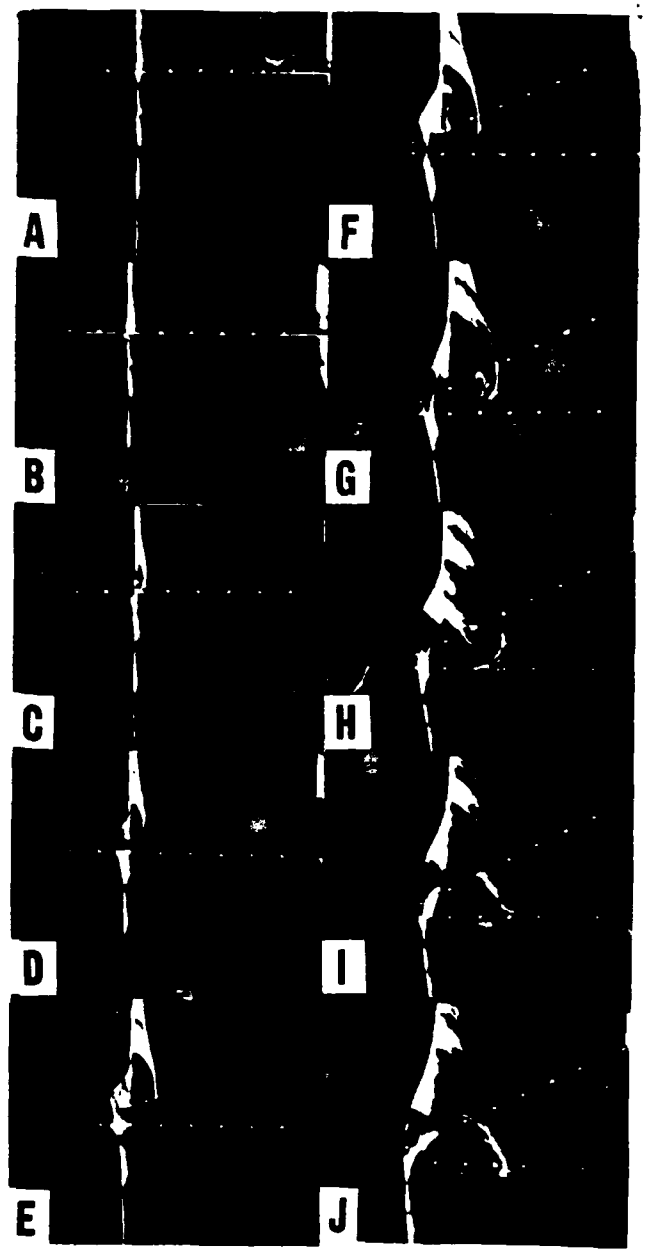


Fig. 9 - $\Lambda 30^{\circ}$; $\alpha^{+}$1.0; $c_r$ 0.4; $\Delta\bar{\epsilon}$ 0.2

Effect of Non-dimensional Pitch Rate

The nondimensional pitch rate primarily affected the residence time of the vortex over the wing surface. Figures 2, 10, and 11 show side views of the 30° delta wing for nondimensional pitch rates of 1.0, 0.6, and 0.2 respectively. Photographs A through J have been arranged at equivalent angles of attack between figures. For example, plate D shows the 30° delta at an angle of attack of 20° for all three figures.

Similar to previous two-dimensional results, the vortex remained over the wing at higher angles of attack with increasing pitch rates. At $\alpha^{+}$ of 0.2, the vortex is resident in Figure 11D ( $\alpha$ = 26°) and has shed by 11E. The presence of a coherent vortex is extended to 58° for $\alpha^{+}$ = 0.6 (Figure 10G), and for $\alpha^{+}$ = 1.0 (Figure 2H). Concurrently, the vortex remained more coherent and achieved a larger diameter with increasing pitch rate.

Although greater angles were achieved, the actual duration time of the vortex over the delta wing diminished with increasing pitch rate. Figure 12 shows the increase in vortex diameter as a function of both nondimensional time (left) and angle of attack (right). The three plates from top to bottom show increasing pitch rates of 0.2, 0.6, and 1.0 respectively. The nondimensional time range for which data is plotted indicates a measure of the vortex duration over the wing. On each plate, the vortex development was plotted at various span locations correlating to the streakline visualizations made for different planes of smoke injection. For selected span locations, the angle of attack attained before vortex breakdown occurred increased from 25° at $\alpha^{+}$ = 0.2 to over 50° at $\alpha^{+}$ = 1.0. The same data plotted with respect to nondimensional time (left column) indicates that the duration of the vortex residence actually decreased by a factor of 2.0 when the pitch rate was increased from 0.2 to 1.0. Although this figure shows only the data for the 45° delta

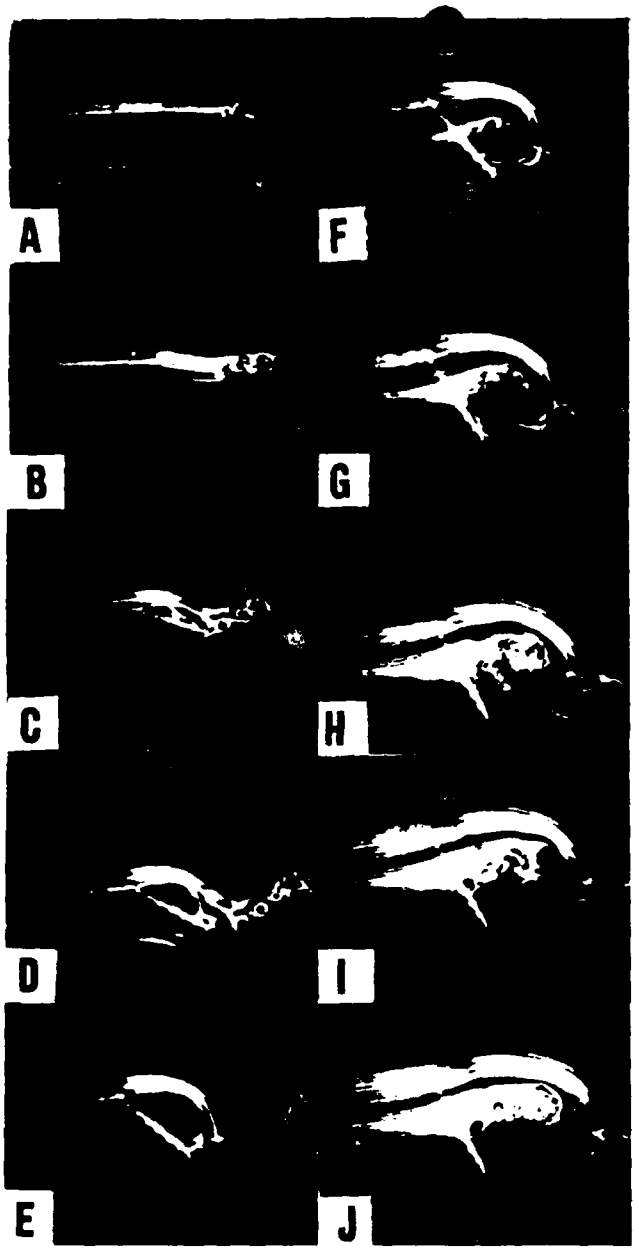


Fig. 10 - $\Lambda 30^{\circ}$; $\alpha^{+} 0.6$; $c_r$ 0.8; $\Delta\bar{t}$ 0.3;

wing, similar trends were noted for the 30° and 60° deltas.

Unlike previous two-dimensional airfoil results, higher pitch rates did not appear to delay the onset of vortex initiation. A threshold condition of between 8 and 10 degrees angle of attack was observed to be the limiting criteria for vortex initiation, independent of pitch rate. These same threshold angles were evident in the 30° and 60° delta wing data as well. Leading edge vortices also begin to develop on delta wings in steady flow at approximately these same values.

The variable growth rate of the leading edge vortex over the delta wing is also evident in Figure 12. Immediately after vortex initiation, the vortex diameter appeared fairly uniform along the leading edge of the wing. As the vortex continued to develop, the diameter near the tip (outboard) developed at a more rapid rate than near the root resulting in a somewhat conical vortex

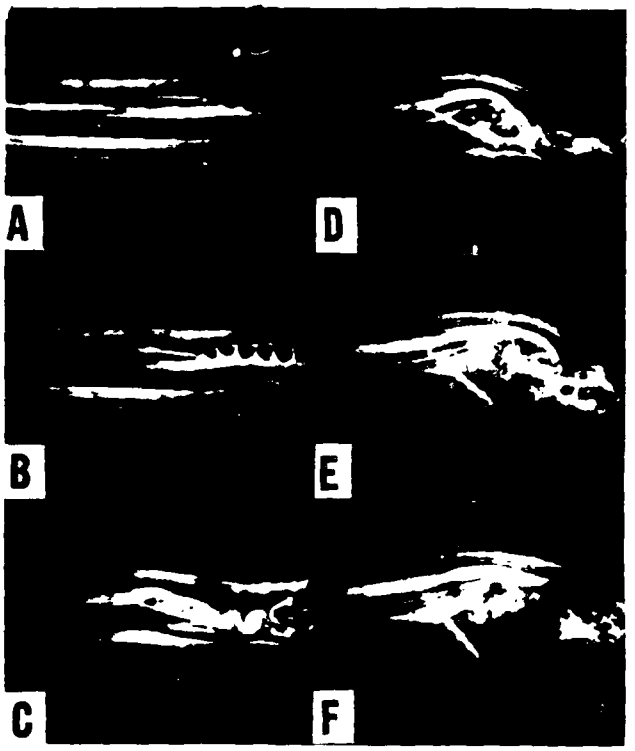


Fig. 11 - $\Lambda 30^{\circ}$; $\alpha^{+} 0.2$; $c_r$ 0.8; $\Delta\bar{t}$ 1.0;

shape. The growth rates along the span varied with changes in pitch rate and planform. These growth rates did not show a strong correlation to either nondimensional time or angle of attack.

Miscellaneous Observations

Two other interesting events were seen in the flow visualization films. The first was a strong periodic entrainment of smoke at inboard locations into the vortex that was developing along the leading edge at more outboard locations. This entrainment is clearly shown in Figure 13. The vortex that exists outboard of the smoke sheet is pulling the smoke across the upper surface, very effectively dominating the flow field over a region much larger than the actual extent of the vortex itself. The appearance of periodicity in the entrained flow was not consistent but was observed to be more prevalent at $\alpha^{+} = 0.2$ on the 60° delta wing than elsewhere.

Figure 13 also shows a leading edge vortex that is laminar at inboard locations, but very quickly becomes turbulent while still aligned with the leading edge. This sudden transition is accompanied by a dramatic increase in vortex size. These characteristics are indicative of the vortex burst phenomenon often seen over delta wings in steady flow. Measurements of flow velocities would be useful in determining if, in fact, this is a vortex burst, but the appearance and the conditions of occurrence would indicate so. The sudden change in vortex character was observed only on the 60° delta wing. If it is a bursting vortex , the occurrence at 60° would support previous hypotheses that the swirl content of the vortex, created by substantial flow velocity along the axis of the vortex, is a critical factor in producing vortex burst.

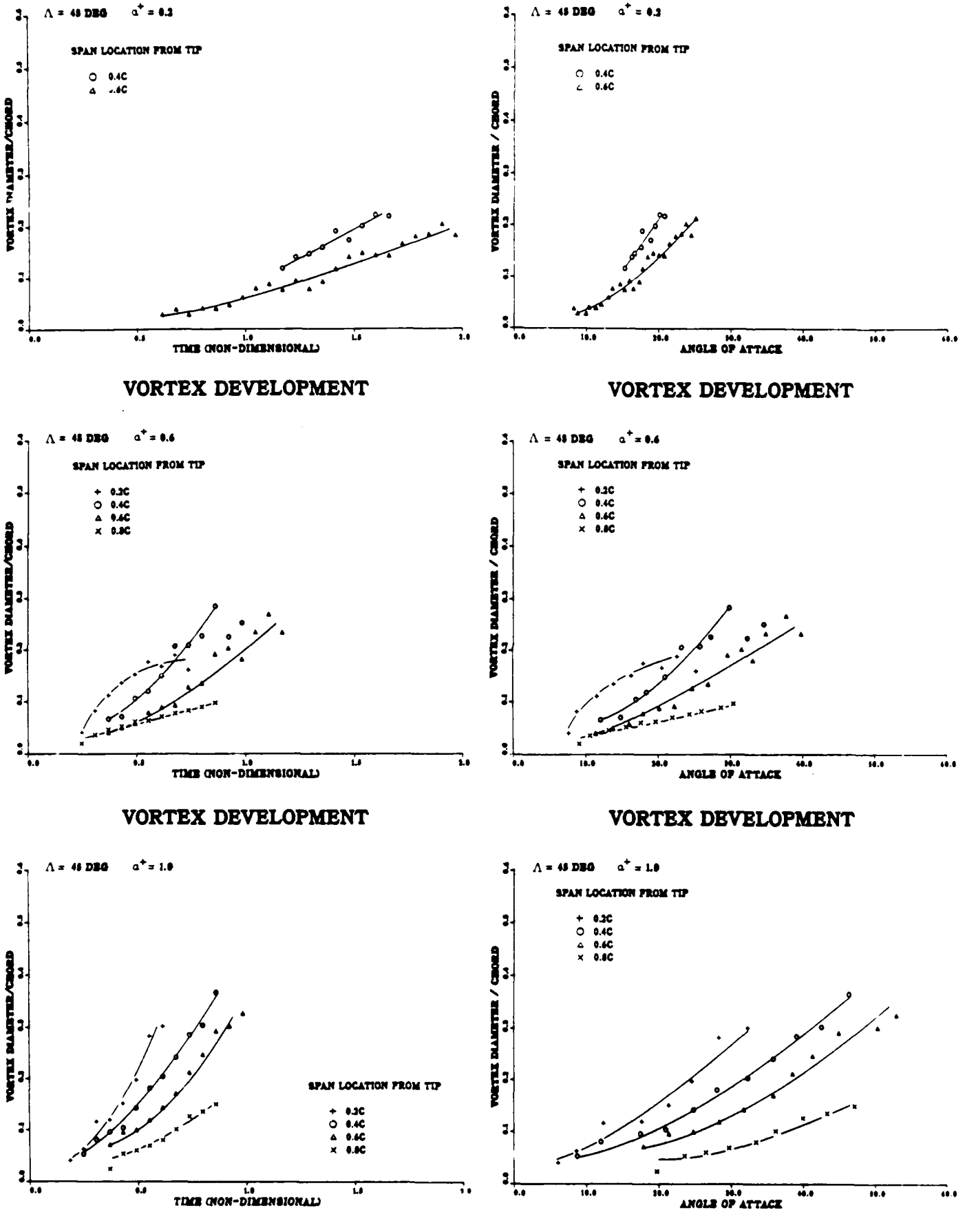


Fig. 12 - Vortex development over a 45° delta wing;

Fig. 13 - Flow entrainment over a 60° delta wing; Λ60°; $\alpha^+$ 0.2; $c_r$ 1.2;

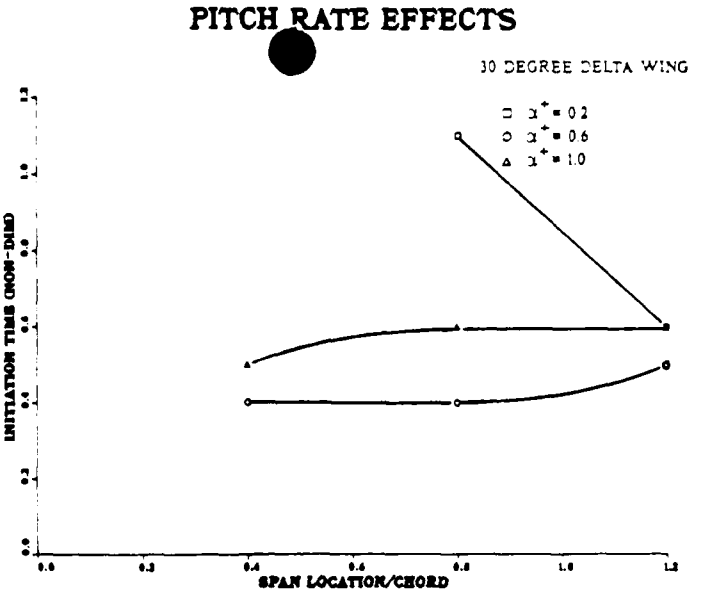


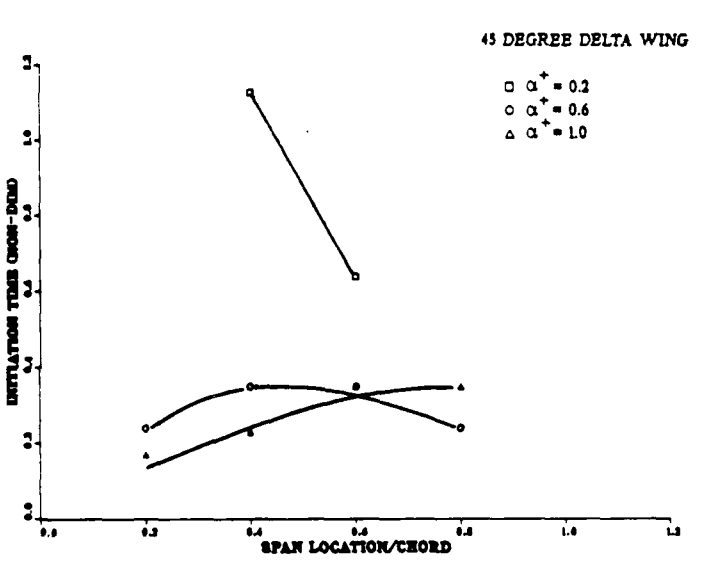


Fig. 14 - Vortex initiation along the span.

## Discussion

Smoke wire visualizations made at various span locations permitted a rapid global assessment of the flow to be made including three-dimensional effects. This technique proved especially useful when analyzing the flow field effects resulting from alterations in test geometry and motion history. Although qualitative in nature, many quantitative relationships governing the dynamics of vortex development could be resolved from the visualization results.

The vortex initiation and development produced by a delta wing driven with a constant pitch rate motion was similar to the results reported by Gad-el-Hak and Ho using sinusoidal motions through large angles of attack. During the upstroke, a vortex initiates at low angles of attack and grows in diameter with increasing α. With sinusoidal motions, the vortex diameter decreases after the wing reverses pitch direction and moves toward minimum angle. Hence, the flow is continually forced through all portions of the cycle by the continual motion. In contrast, the constant pitch motion is divided into a forcing period where vortex initiation occurs and a relaxation phase where wing motion ceases and the vortex develops in an unforced environment. Whereas the initiation and initial development are similar to the sinusoidal motion, the constant pitch motion drives the occurrence of full vortex development to very high angles of attack. Depending upon test conditions, the developed vortex separates from the delta wing and rapidly breaks down into an incoherent structure and/or convects away.

Vortex initiation along the delta wing leading edge was observed to depend upon both planform geometry and nondimensional pitch rate. Figure 14 plots the nondimensional time for vortex initiation along the delta wing span as a function of span location and nondimensional pitch rate. The two separate plates indicate the initiation for the 30° and 45° delta wings. For higher nondimensional pitch rates (0.6, 1.0) the vortex initiates slightly earlier in the pitch cycle at span locations near the tip and progresses toward the root. This observation, as noted earlier, is consistent with previously published results. (18,22)

At the lowest value of nondimensional pitch rate tested (0.2), this trend is reversed with separation occurring first near the root chord and moving toward the tip. Near the tip ( $0.4c_r$ ) the leading edge vortex failed to initiate at all. The obvious discrepancy between high and low pitch rates indicates that a fundamental difference in the in the vortex initiation and development processes was occurring between these test conditions. For all tested geometries, the sharp leading edge of the delta wing "fixed" the separation point for vortex initiation. At high pitch rates, vortex initiation is temporally "localized" due to the rapid change in angle of attack through the separation angle. These high rates result in discernible vortex initiation along

the entire span of the leading edge from root to tip. After initiation, high pitch rates promote a more rapid growth in vortex diameter along the span. In contrast, visualization results of the low pitch rates show a less dynamic initiation and development. Separated flow near the delta wing tip fails to organize into the tightly helical shape observed with higher pitch rates. Instead, the separated shear layer moves away from the leading edge inboard from the tip. A more gradual roll up of this shear layer produces a vortex nearly aligned with the freestream velocity vector rather than with the delta wing leading edge. Thus, a clearly defined vortex never forms at the tip. This capricious vortex initiation was evident for all three delta wings at the low pitch rate.

The mechanisms through which longer duration vortices are promoted are not understood. It is, however, readily apparent that lower pitch rates clearly sustain vortex residence for appreciable periods of time independent of planform geometry. These results are also consistent with the lower vortex convection rates observed when two-dimensional airfoils are driven with low pitch rates. The strong interdependence between the angle of attack achieved at higher pitch rates and an earlier vortex demise may provide some insight into the vortex breakdown phenomena.

## Conclusions

Delta wings driven with constant pitch rate motions have been shown to produce large scale vortical formations similar to those observed in previous studies using sinusoidal oscillations. Following initiation, however, subsequent development differed from sinusoidal results in that the leading edge vortex was not stationary on the wing, but dominated the upper wing surface flow field for a period before breaking up and/or convecting away from the wing. In this global development sense, the flow field resembled that for a two-dimensional airfoil or a straight three-dimensional wing driven with constant pitch rate motions.

The three-dimensional delta wing planform elicited a complicated wake pattern dependent upon both sweep angle and nondimensional pitch rate. Vortex duration over the wing surface varied inversely with nondimensional pitch rate. However, the angle to which the wing could be driven with a coherent vortex in residence increased directly and dramatically with nondimensional pitch rate. Duration was also a function of span position with inboard locations achieving higher durations independent of pitch rate or wing planform effects. Vortex growth rate was a maximum at the most outboard span positions and steadily decreased for positions nearer the root.

Smoke wire visualization permitted detailed assessments to be made of the flow characteristics including three-dimensional effects. Although complex, the flow structures produced were repeatable and well defined. Findings, thus far, are very enlightening. However, a more comprehensive investigation will be required in order to fully determine the character of the complex three-dimensional flow field and its dependency on wing planform and pitch parameters.

## References


1. McCroskey, W.J., "Unsteady Airfoils", Annual Review of Fluid Mechanics, 1982, pp 285-311.

2. McCroskey, W.J., "Some Current Research in Unsteady Fluid Mechanics", The 1976 Freeman Scholar Lecture, J. Fluids Engineering, Vol 99, 1977, pp 8-38.

3. Carr, L.W., "Dynamic Stall -- Progress in Analysis and Prediction", AIAA Paper 85-1769, Snowmass, CO, Aug 1985, pp 1-33.

4. Robinson, M.C. and Luttges, M.W., "Unsteady Flow Separation and Attachment Induced by Pitching Airfoils", AIAA Paper 83-0131, Reno NV, Jan 1985, pp 1-12.

5. Robinson, M.C. and Luttges, M.W., "Vortex Generation Induced by Oscillating Airfoils; Maximizing Flow Attachment", VIII Biennial Symposium on Turbulence, University of Missouri, Rolla MO, 1983, pp117-126.

6. Robinson, M.C. and Luttges, M.W., "Unsteady Separated Flow: Forced and Common Vorticity about Oscillating Airfoils", Workshop on Unsteady Separated Flows, Francis, M. and Luttges, M. (eds.), Univ of Colorado, Boulder CO, 1983, pp 117-126.

7. McAlister, K.W., and Carr, L.W., "Water Tunnel Visualizations of Dynamic Stall", Jour. Fluids Engr., Vol 101, 1979, pp376-380.

8. McCroskey, W.J., Carr, L.W., and McAlister, K.W., "Dynamic Stall Experiments on Oscillating Airfoils", AIAA Paper 75-125, Jan 1975.

9. Carr, L.W., McAlister, K.W., and McCroskey, W.J., "Analysis of the Development of Dynamic Stall Based on Oscillating Airfoil Experiments", NASA TN-8382, Jan 1977.

10. Walker, J.M., Helin H.E., and Strickland, J.H., "An Experimental Investigation of an Airfoil Undergoing Large Amplitude Pitching Motions", AIAA Journal, Vol 23, Aug 1985, pp 1141-1142.

11. Walker, J.M., Helin, H.E., and Chou, D.C., "Unsteady Surface Pressure Measurements on a Pitching Airfoil", AIAA Paper 85-0532, Boulder CO, Mar 1985.

12. Francis, M.S., and Keesee, J.E., "Airfoil Dynamic Stall Performance with Large Amplitude Motions", AIAA Journal, Vol 23, Nov 1985, pp 1653-1659.

13. Robinson, M.C., and Luttges, M.W., "Vortices Produced by Air Pulse Injection from the Surface of an Oscillating Airfoil", AIAA Paper 86-0118, Reno NV, Jan 1986.

14. Luttges, M.W., Robinson, M.C., and Kennedy, D.A., Control of Unsteady Separated Flow Structures on Airfoils", AIAA Paper 85-0531, Boulder CO, Mar 1985, pp 1-12.

15. Helin, H.E., Robinson, M.C., and Luttges, M.W., "Visualization of Dynamic Stall Controlled by Large Amplitude Interrupted Pitching Motions", AIAA Paper 86-2281-CP, Williamsburg VA, Aug 1986.

16. Viets, H., Palmer, M.G., and [redacted]hke, R.J., "Potential Applications of Forced Unsteady Flows", Workshop on Unsteady Separated Flows, Francis, M. and Luttges, M. (eds.), Univ of Colorado, Boulder CO, 1983, pp 21-27.

17. Adler, J.N., and Luttges M.W., "Three-Dimensionality in Unsteady Flow About a Wing", AIAA Paper 85-0132, Reno NV, Jan 1985.

18. Gad-el-Hak, M., and Ho, C.-M., "The Pitching Delta Wing", AIAA Journal, Vol 23, Nov 1985.

19. Ashworth, J., Waltrip, M., and Luttges, M.W., "Three-Dimensional Unsteady Flow Fields Elicited by a Pitching Forward Swept Wing", AIAA Paper 86-1104, Atlanta GA, May 1986.

20. Robinson, M., Helin, H., Gilliam, F., Russell, J., and Walker, J., "Visualization of Three-Dimensional Forced Unsteady Flow", AIAA Paper 86-1066, Atlanta GA, May 1986.

21. Jumper, E.J., Shreck, S.J., and Dimmick, R.L., "Lift Curve Characteristics for an Airfoil Pitching at Constant Rate", AIAA Paper 86-0117, Reno NV, Jan 1986.

22. Gad-el-Hak, M., and Ho, C.-M., "Unsteady Vortical Flow Around Three-Dimensional Lifting Surfaces", AIAA Journal, Vol 24, May 1986.